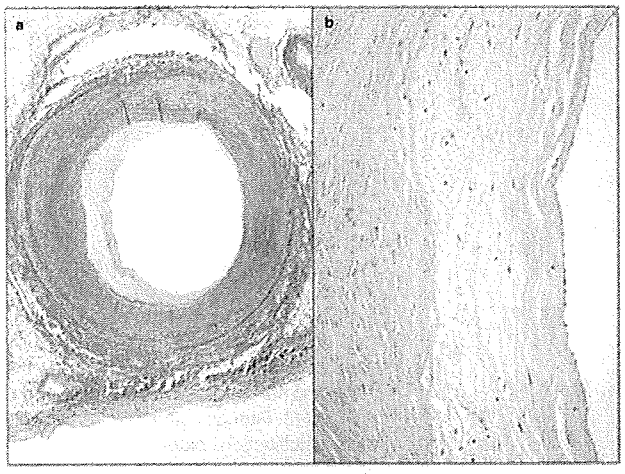

Figure 6 Distal region of the LAD stent (just distal of the stent). Concentric fibrotic thickening of the intima is seen, but there is almost no inflammatory cell infiltration. (a: EvG stain, b: HE stain).

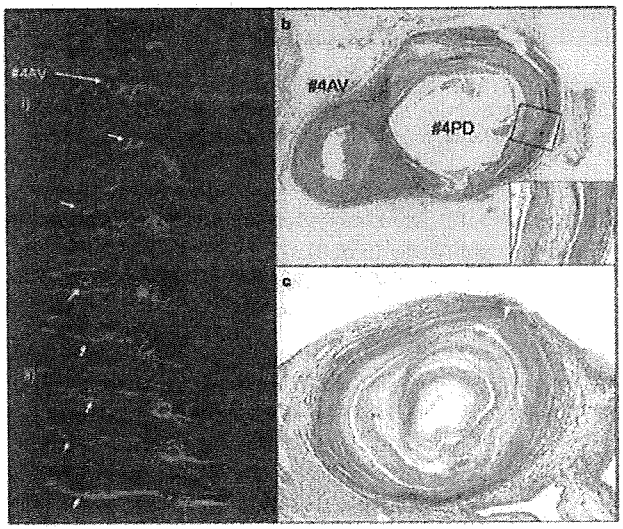

Figure 7 RCA #4. (**a**) Cross-sections. An aneurysm is seen to have formed at #4PD, and at its end the intima is observed to be narrowed due to the presence of an organized thrombus. (**b**) The region shown in Fig. 7a)-i). The histological findings for the aneurysm at #4PD are almost the same as those for the LAD aneurysm. Focal mural thrombi were seen at #4PD and #4AV. (EvG stain) (inset: Magnification of the aneurysm wall. Hyalinized intimal thickening accompanied by calcification, extension of internal elastic lamina and thinning of the tunica media are seen. (**c**) The region shown in Fig. 7a)-ii). The intima is almost completely obliterated by an organized thrombus. (EvG stain).

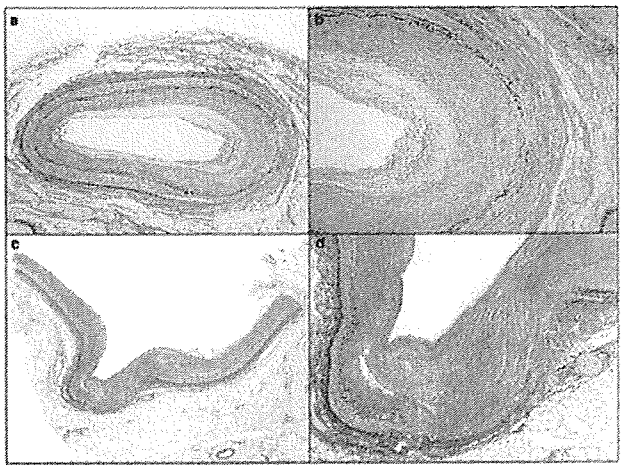

Figure 8 Photomicrograph of the sites of the coronary arteries which showed no aneurysmal dilation. (**a,b**) LCx #12. Diffuse concentric fibro-cellular intimal thickening, partial disruption of the internal elastic lamina and thinning tendency of the tunica media were seen. (EvG stain). (**c,d**) Although the basic structure of artery was kept, a diffuse concentric fibro-cellular intimal thickening was seen in RCA #1. In addition, scarring of arteritis with complete destruction of vascular structure was observed at its branching site.

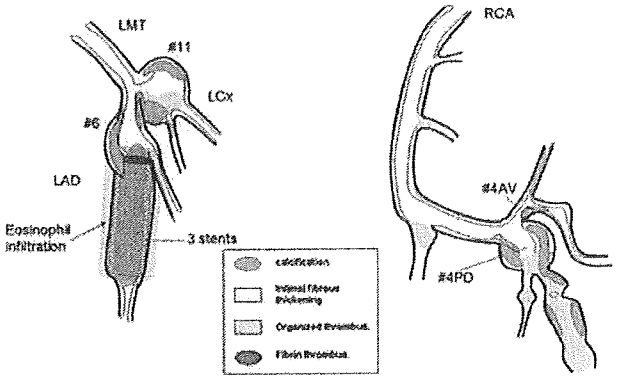

Figure 9 Schema of the changes observed in the coronary arteries. In the left coronary artery, aneurysms had formed at LCx #11 and LAD #6. Three stents had been implanted in the distal portion of the aneurysm in LAD #6. The lumen of each stent was occluded with a fibrin thrombus and extensive infiltration by eosinophils. The right coronary artery showed a coronary aneurysm at #4PD.

disease and polyarteritis nodosa. Because the arterial changes observed in this patient were only images of scarring, it was impossible to find any acute inflammatory changes. Takahashi *et al.*[12] reported that the wall of coronary artery aneurysms in the remote stage of Kawasaki disease consisted of hyalinized dense fibrous tissue accompanied by lamellar calcification, and that a concentric intimal thickening, extension of internal elastic lamina and a thinning of the tunica media were observed even in the coronary arteries with no aneurysm formation. These histological findings closely resemble those of this patient. Furthermore, the lesions were only seen in the coronary arteries, with no lesions in the arteries in other organs such as the kidney or pancreas. From the perspective of distribution of vascular lesions, it was surmised that the findings were strongly supportive of these coronary artery changes' being remote

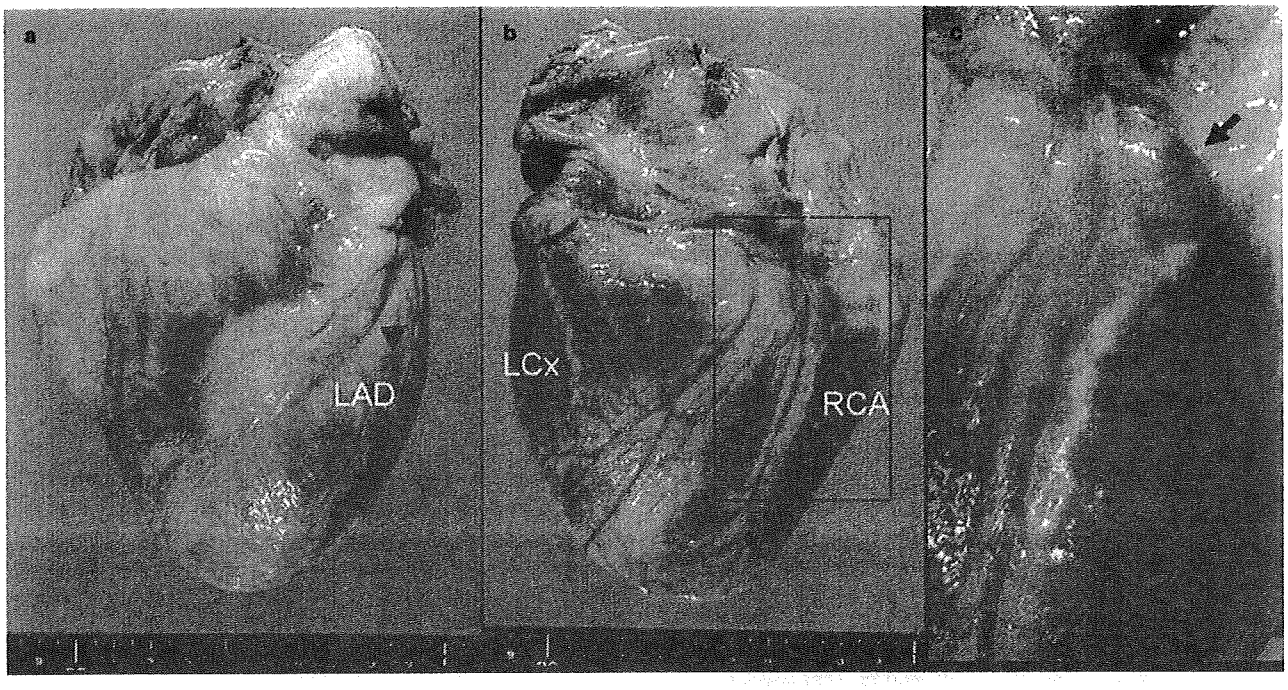

Figure 2 Gross images of the heart. (**a**) Anterior view. Whitish, rigid changes due to calcification are seen in part of the LAD (arrow head). (**b**) Posterior view. An aneurysm is seen a RCA #4. (**c**) Magnification of (**b**). Formation of a saccular aneurysm having a diameter of approximately 7 mm is seen (arrow), and the end (arrow head) of the aneurysm is rigid and serpentine due to calcification.

the stent. And then, the tissues were embedded in paraffin, and Hematoxylin and eosin stain, Elastica van Gieson stain, Azan-Mallory stain were performed for routine histological examination. Fibrocellular neointimal thickening had formed above the BMS stent strut, but the surface of the DES stent strut was not covered with any neointima and a thrombus was adhered to it. The lumen of each stent was occluded with a poorly organized fibrin thrombus, and extensive infiltration by inflammatory cells was observed in the thrombus and all layers of the vascular wall (Fig. 5). The inflammatory cells were predominantly eosinophils, with smaller numbers of lymphocytes, plasma cells and foreign-body-type giant cells. This striking eosinophil infiltration was confined to the site of implantation of the stents, and no infiltration by inflammatory cells, including eosinophils, was observed in either the aneurysmal wall on the proximal side (Fig. 4c) of the stents or the arterial wall on the distal side (Fig. 6) thereof.

Inspection of the RCA showed a coronary aneurysm having a diameter of approximately 7 mm and accompanied by calcification in the aneurysmal wall at #4PD, with organized thrombotic occlusion peripheral thereto (Fig. 7). Focal mural thrombi were seen at #4AV and #4PD, but no eosinophil infiltration was observed.

Concerning the sites of the coronary arteries which showed no aneurysmal dilation, diffuse concentric intimal thickening, extension and focal rupture of the internal elastic lamina and focal destruction of the tunica media were also observed (Fig. 8). The changes in the coronary arteries are depicted schematically (Fig. 9).

With regard to the aorta, only very slight fibrotic thickening of the intima was seen, and there were few atherosclerotic changes and no rupture of the internal elastic lamina or degeneration of the tunica media. Almost no changes were observed in the other arteries of the body.

DISCUSSION

At the time of the first episode of acute myocardial infarction in this patient, a BMS was implanted at LAD #7. Thereafter, in spite of administration of suitable antiplatelet therapy, she experienced five episodes of stent occlusion during the 28-month period until her sudden death. At 16 months and also at 2 years after the implantation of the BMS, a DES was implanted so that each would overlap the BMS. The patient died 5 months after the implantation of the second DES. The autopsy revealed thrombi in the stents and a profound degree of eosinophil infiltration that coincided with the sites of stent implantation. It was surmised that a hypersensitivity reaction in relation to the stent had been involved in the LST. There have been few published reports of autopsy findings indicating occurrence of a hypersensitivity reaction caused by a stent. It was reported that lymphocytes, macrophages and foreign-body-type giant cells are seen in the vicinity of

Advance Publication by J-STAGE

Circulation Journal
Official Journal of the Japanese Circulation Society
http://www.j-circ.or.jp

Lipocalin-2/Neutrophil Gelatinase-B Associated Lipocalin is Strongly Induced in Hearts of Rats With Autoimmune Myocarditis and in Human Myocarditis

Limin Ding, MD; Haruo Hanawa, MD; Yoshimi Ota, PhD†; Go Hasegawa, MD*; Kazuhisa Hao, MD; Fuyuki Asami, MD**; Ritsuo Watanabe, MD; Tsuyoshi Yoshida, MD; Ken Toba, MD; Kaori Yoshida, BS; Minako Ogura, BS; Makoto Kodama, MD; Yoshifusa Aizawa, MD

Background: Lipocalin-2/neutrophil gelatinase-B associated lipocalin (Lcn2/NGAL) is involved in the transport of iron and seems to play an important role in inflammation. A recent study has reported that it is also expressed in the failing heart and may be a biomarker not only for renal failure but also for heart failure. Because Lcn2/NGAL is thought to be induced by interleukin-1, it might be strongly induced in the presence of myocarditis.

Methods and Results: This study investigated the expression of Lcn2/NGAL in rat experimental autoimmune myocarditis (EAM) and in human myocarditis. In EAM hearts, the expression of Lcn2/NGAL was markedly increased (>100-fold at an early stage), and in human myocarditis it was also highly expressed compared with non-inflammatory failing hearts. Lcn2/NGAL expressing cells in hearts with EAM and human myocarditis were identified as cardiomyocytes, vascular wall cells, fibroblasts and neutrophils. Lcn2/NGAL in EAM rats was also expressed in the liver. Plasma Lcn2/NGAL levels abruptly increased at an early stage of EAM, and high levels were initially sustained during the inflammatory stage, then decreased with recovery. In contrast, levels of B-type natriuretic peptide increased only slowly as the disease progressed.

Conclusions: Cardiomyocytes, vascular wall cells and fibroblasts in myocarditis strongly express Lcn2/NGAL via proinflammatory cytokines.

Key Words: Biomarker; Cardiomyopathy; Cytokine; Myocarditis; Reactive oxygen species

Lipocalin-2/neutrophil gelatinase-B associated lipocalin (Lcn2/NGAL) is a protein associated with neutrophil gelatinase,[1] and plays a role as an antibacterial factor.[2] It is suggested that Lcn2/NGAL may play other important roles in inflammation because it is involved in the transport of iron across cell membranes,[3] and is thought also to closely regulate apoptosis.[4] Other recent reports have suggested that Lcn2/NGAL has a protective effect against oxidant stress.[5]

Lcn2/NGAL was initially identified in activated neutrophils, then subsequently shown that many other types of cells, including kidney tubular cells, lung type II alveolar epithelial cells, and liver hepatocytes may produce NGAL in response to injuries.[6,7] Recent investigations of Lcn2/NGAL in renal disease suggest that it may be a promising new biomarker for acute renal failure. It has been speculated that the increase in the Lcn2/NGAL level after renal tubular injury may serve to limit injury in recurrent insults or even ameliorate the degree of damage in an ongoing insult.[7]

Numerous studies have previously reported that Lcn2/NGAL is a biomarker of renal failure associated with heart diseases.[8–11] Those studies demonstrated that urine and serum concentrations of Lcn2/NGAL, which was produced by the proximal tubules, were increased in patients with acute renal failure after cardiac surgery or in chronic heart failure. On the other hand, a few studies have reported that Lcn2/NGAL is expressed also in the heart.[12,13] Lcn2/NGAL was highly expressed in transplanted hearts[12] or following X-ray exposure,[13] and Lcn2/NGAL expressing cells were found to be heart granulocytes.[12] In addition, a recent study has demonstrated that Lcn2/NGAL is produced by cardiomyocytes and resident cells in failing hearts, and might serve as a useful biomarker for heart failure.[14] Our previous study using micro-

Received July 3, 2009; revised manuscript received October 28, 2009; accepted October 29, 2009; released online January 7, 2010
Time for primary review: 12 days

Division of Cardiology, *Division of Cellular and Molecular Pathology, **Department of Thoracic and Cardiovascular Surgery, Niigata University Graduate School of Medical and Dental Sciences and †Department of Medical Technology, School of Health Sciences, Faculty of Medicine, Niigata University, Niigata, Japan

Mailing address: Haruo Hanawa, MD, Division of Cardiology, Niigata University Graduate School of Medical and Dental Sciences, 1-757 Asahimachi-dori, Niigata 951-8120, Japan

ISSN-1346-9843 doi:10.1253/circj.CJ-09-0485

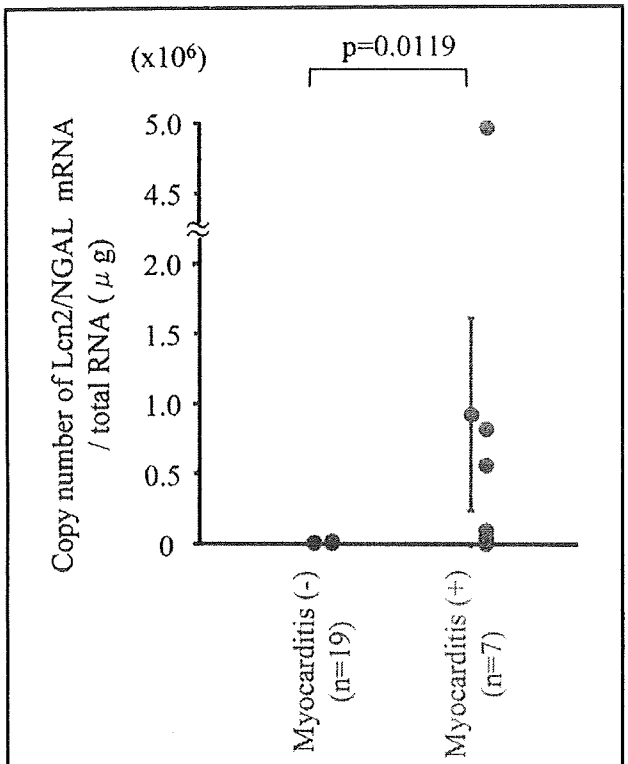

Figure 7. Gene expression of Lcn2/NGAL mRNA in hearts of patients (19 patients without myocarditis and 7 patients with myocarditis). The clinical characteristics of patients were described previously.[21] Error bars represent SEM. Statistical assessment was performed by the Mann-Whitney U test. Lcn2, lipocalin-2; NGAL, neutrophil gelatinase-B associated lipocalin.

thelial cells, pericytes, smooth muscle cells and fibroblasts (Figure 2A). Lcn2/NGAL specific receptor (24p3R) expressing cells were also identified as cardiomyocytes and NCNI cells (Figure 2B).

Time Course of Plasma Lcn2/NGAL, IL-1β, and BNP Levels in EAM

Plasma Lcn2/NGAL levels in EAM rats were significantly increased at day 13 compared with normal rats and control rats injected with adjuvant alone, and the high levels of plasma Lcn2/NGAL continued until day 33 but decreased to the near-normal range after day 45 (Figure 3A). The time course of plasma Lcn2/NGAL was similar to that of Lcn2/NGAL expression in EAM hearts. Plasma IL-1β levels in EAM rats showed an increase at day 9 and were significantly higher than in control rats from day 13 to day 29, but decreased thereafter (Figure 3B). As previously reported for IL-1β-induced Lcn2/NGAL expression, the time course of plasma Lcn2/NGAL was also similar to that of IL-1β. On the other hand, plasma BNP levels in the EAM rats slowly increased after the peak of infiltration by inflammatory cells compared with control rats (Figure 3C) and the time course of plasma BNP differed from that of Lcn2/NGAL.

Analysis of Lcn2/NGAL and IL-1β-Expressing Organs in EAM

Because Lcn2/NGAL expression and plasma Lcn2/NGAL levels in EAM hearts increased significantly on days 12 and 13, respectively, we investigated Lcn2/NGAL expression in the livers, kidneys and spleens of EAM rats at day 13. Lcn2/NGAL mRNA was significantly increased not only in the hearts but also in the livers. Lcn2/NGAL mRNA expression in the kidneys was also increased, but to a lesser degree than in the hearts or livers (Figure 4).

Lcn2/NGAL Immunostaining in Rat and Human Hearts

Lcn2/NGAL immunostaining was hardly detected in normal rat hearts (Figure 5A). In the EAM rat hearts, on the other hand, it was found in cardiomyocytes (Figure 5B-1), vascular wall cells (Figure 5B-2), spindle-like fibroblastoid cells and leukocytes (Figure 5B-3). In the heart of Case 1 with primary pulmonary hypertension, Lcn2/NGAL immunostaining was not detected (Figure 6A); however, in the hearts of Cases 2–4 with myocarditis, it was found in cardiomyocytes (Figures 6B, C, D-1, D-2), vascular wall cells (Figure 6D-2), spindle-like fibroblastoid cells and leukocytes (Figure 6D-3).

Western Blot Analysis of Lcn2/NGAL in Human Hearts

In the heart of Case 1 with primary pulmonary hypertension, Lcn2/NGAL protein in the heart was hardly detected by Western blot analysis, but was detected in the hearts of Cases 2 and 3 (Figure 6E).

Lcn2/NGAL mRNA Expression in Human Hearts

Lcn2/NGAL mRNA levels in human hearts with myocarditis measured by real-time RT-PCR were significantly greater than in those without myocarditis (Figure 7). However, as shown in our recent studies,[21] there was no significant difference in BNP mRNA levels.

Discussion

Recently Yndestad et al[14] reported that Lcn2/NGAL is highly expressed in the cardiomyocytes of heart failure patients, and might be a useful biomarker of the severity of heart failure. In the current study we demonstrated that Lcn2/NGAL expression in the hearts of rats and humans with myocarditis, as well as the plasma Lcn2/NGAL levels in EAM rats, were significantly increased compared with normal or control rats. However the increase in Lcn2/NGAL in our study was more pronounced than in the study of Yndestad et al.[14] Moreover, our time course analysis in EAM rats showed that elevation of both the cardiac expression of Lcn2/NGAL and of the plasma Lcn2/NGAL level was more marked during the active stages of myocarditis, and closely paralleled cardiac IL-1β expression levels and plasma IL-1β levels. Yndestad et al demonstrated that IL-1-induced Lcn2/NGAL expression occurs in rat neonatal cardiomyocytes, and we made similar observations (data not shown). Interleukins like IL-1 usually act in an autocrine/paracrine fashion, not in an endocrine fashion. Collectively these observations suggest that Lcn2/NGAL expression in hearts is markedly increased, in synchrony with the timing of elevation of cytokines such as IL-1 in the heart.

Lcn2/NGAL is a novel protein involved in iron transport.[4] In the current study, its specific receptor (24p3R) was also expressed in cardiomyocytes and NCNI cells. We therefore hypothesized that Lcn2/NGAL acts in an autocrine fashion. Cardiomyocytes possess considerable amounts of protein, including an abundance of iron-containing myoglobin and ferritin.[23,24] When cardiac injury occurs, iron is thought to be dispersed within the extracellular space of the heart.

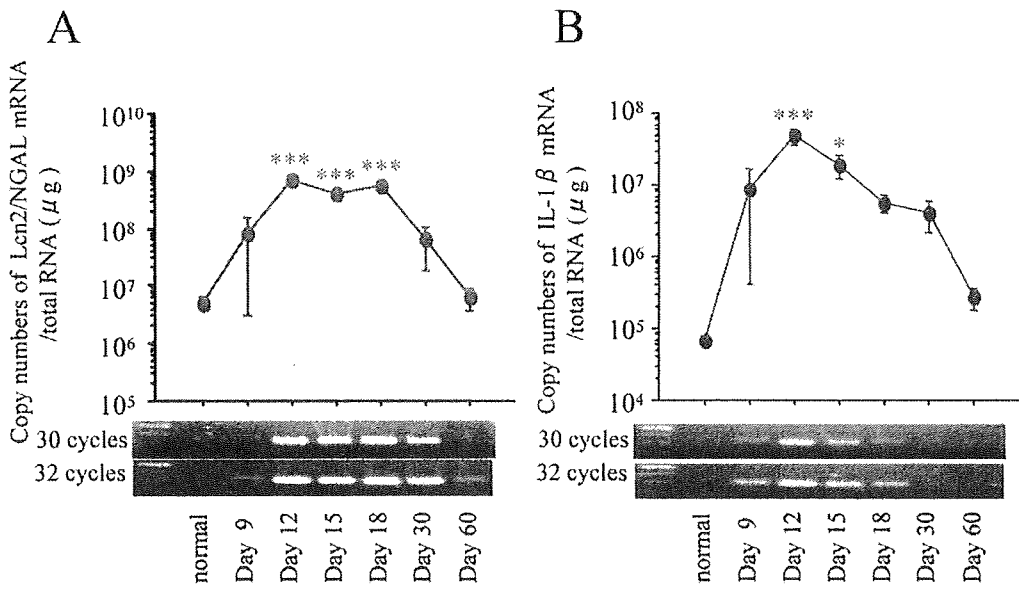

Figure 1. Time course of gene expression of Lcn2/NGAL (A) and IL-1β (B) in normal (n=3) and EAM hearts on day 9, 12, 15, 18, 30 (n=3 for each), and 60 (n=4). PCR bands after 30 and 32 cycles were visualized by ethidium bromide. Error bars represent SEM. Statistical assessment was performed by 1-way ANOVA and Bonferroni's multiple comparison test. Significant differences between normal (8-week old rats without adjuvant injection) and other groups are shown. Differences were considered significant at P<0.05. ***P<0.001 vs normal rat; **P<0.01 vs normal rat; *P<0.05 vs normal rat. EAM, experimental autoimmune myocarditis; IL-1, interleukin-1; Lcn2, lipocalin-2; NGAL, neutrophil gelatinase-B associated lipocalin; PCR, polymerase chain reaction.

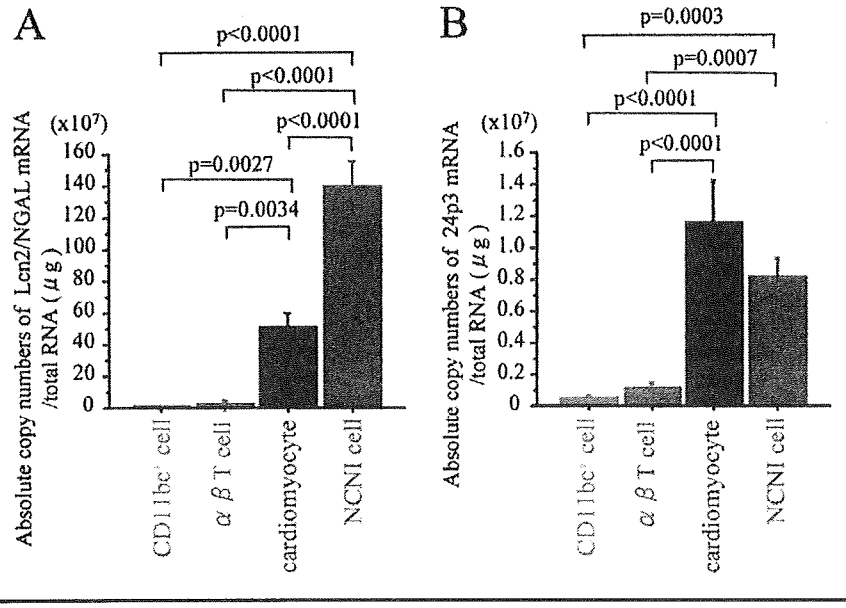

Figure 2. Gene expression of Lcn2/NGAL (A) and 24p3R (B) in each cell fraction from EAM hearts. Fractions of CD11bc⁺ cells (n=5), αβ T cells (n=5), cardiomyocytes (n=5) and NCNI (n=6) were separated and purified from EAM hearts on day 18. NCNI cells were mainly fibroblasts, smooth muscle cells and endothelial cells. Error bars represent SEM. Statistical assessment was performed by 1-way ANOVA and Bonferroni's multiple comparison test. EAM, experimental autoimmune myocarditis; Lcn2, lipocalin-2; NGAL, neutrophil gelatinase-B associated lipocalin; NCNI, non-cardiomyocytic non-inflammatory.

ary antibody (Nichirei, Tokyo, Japan). After this the specimens were carefully washed 3 times with PBS between each step of the procedure. Finally, they were visualized with 0.1 mg/ml 3,3'-diaminobenzidine (DAB) tetrahydrochloride (Dojin Chemical, Kumamoto, Japan), and counterstained with Mayer's hematoxylin.

Electrophoresis and Western Blot Analysis

Lysates from autopsied human hearts were prepared, and equal amounts (40 μg) of denatured proteins were loaded and separated on 16.5% SDS-PAGE (Mini Protean II; Biorad), and transferred to polyvinylidene difluoride membranes. The membranes were blocked with 10% dry milk in Tris-buffered saline (TBS) for 1 h. Lcn2/NGAL protein was determined by incubation with 1:1,000 rat anti-human Lcn2/NGAL antibody (R&D Systems Inc, Minneapolis, MN, USA) overnight in TBS at 4°C. Membranes were washed 3 times in TBS with 0.05% Triton X-100, followed by incubation for 1 h with

lesions of Kawasaki disease rather than polyarteritis nodosa.[12,13]

In summary, we encountered a case of a young Japanese woman who had undergone stent implantation and then experienced repeated episodes of ST, leading to death, and in whom autopsy revealed an underlying presence of scarring thought to be due to vasculitis associated with Kawasaki disease. The first episode of acute myocardial infarction was surmised to have been due to thrombus formation as a result of a coronary aneurysm. However, the cause of the ST at the time of death was thought to be not only the presence of coronary aneurysms but also a strong hypersensitivity reaction to the stents. Ishii *et al.*[14] reported that catheter intervention was effective for ischemic heart disease manifesting late after Kawasaki disease. Because the lesions of Kawasaki disease show a high degree of calcification, it has been written that rotational ablation is the optimal intervention,[15] while stent implantation is sometimes a treatment arm in the case of stenotic lesions with mild calcification. In general, stent implantation for dilated lesions like coronary artery aneurysms may involve problems such as an increased tendency for thrombus formation and incomplete stent apposition of a stent strut, which are considered to be a potential cause of post-implantation thrombotic occlusion. We conclude that it is essential to exercise caution with regard to stent implantation for ischemic heart disease for which the cause can be thought to have been thrombus formation due to coronary aneurysm(s).

REFERENCES

1 Cutlip DE, Baim DS, Ho KK *et al.* Stent thrombosis in the modern era: A pooled analysis of multicenter coronary stent clinical trials. *Circulation* 2001; **103**: 1967–71.

2 Moreno R, Fernandez C, Hernandez R *et al.* Drug-eluting stent thrombosis: Results from a pooled analysis including 10 randomized studies. *J Am Coll Cardiol* 2005; **45**: 954–9.

3 Daemen J, Wenaweser P, Tsuchida K *et al.* Early and late coronary stent thrombosis of sirolimus-eluting and paclitaxel-eluting stents in routine clinical practice: Data from a large two-institutional cohort study. *Lancet* 2007; **369**: 667–78.

4 Farb A, Weber DK, Kolodgie FD, Burke AP, Virmani R. Morphological predictors of restenosis after coronary stenting in humans. *Circulation* 2002; **25**: 2974–80.

5 Virmani R, Kolodgie FD, Farb A. Drug-eluting stents: Are they really safe? *Am Heart Hosp J* 2004; **2**: 85–8.

6 Virmani R, Guagliumi G, Farb A *et al.* Localized hypersensitivity and late coronary thrombosis secondary to a sirolimus-eluting stent: Should we be cautious? *Circulation* 2004; **109**: 701–5.

7 Nebeker JR, Virmani R, Bennett CL *et al.* Hypersensitivity cases associated with drug-eluting coronary stents: A review of available cases from the Research on Adverse Drug Events and Reports (RADAR) project. *J Am Coll Cardiol* 2006; **47**: 175–81.

8 Kawano H, Koide Y, Baba T *et al.* Granulation tissue with eosinophil infiltration in the restenotic lesion after coronary stent implantation. *Circ J* 2004; **68**: 722–3.

9 Slungaard A, Vercellotti GM, Tran T, Gleich GJ, Key NS. Eosinophil cationic granule proteins impair thrombomodulin function. A potential mechanism for thromboembolism in hypereosinophilic heart disease. *J Clin Invest* 1993; **91**: 1721–30.

10 Wang JG, Mahmud SA, Thompson JA, Geng JG, Key NS, Slungaard A. The principal eosinophil peroxidase product, HOSCN, is a uniquely potent phagocyte oxidant inducer of endothelial cell tissue factor activity: A potential mechanism for thrombosis in eosinophilic inflammatory states. *Blood* 2006; **107**: 558–65.

11 Koster R, Vieluf D, Kiehn M *et al.* Nickel and molybdenum contact allergies in patients with coronary in-stent restenosis. *Lancet* 2000; **356**: 1895–7.

12 Takahashi K, Oharaseki T, Naoe S. Pathological study of postcoronary arteritis in adolescents and young adults: With reference to the relationship between sequelae of Kawasaki disease and atherosclerosis. *Pediatr Cardiol* 2001; **22**: 138–42.

13 Takahashi K, Oharaseki T, Yokouchi Y, Naoe S, Jenneette JC. Kawasaki disease arteries and polyarteritis nodosa. *Pathology Case Reviews* 2007; **12**: 193–9.

14 Ishii M, Ueno T, Ikeda H *et al.* Sequential follow-up results of catheter intervention for coronary artery lesions after Kawasaki disease: Quantitative coronary artery angiography and intravascular ultrasound imaging study. *Circulation* 2002; **105**: 3004–10.

15 Akagi T. Interventions in Kawasaki disease. *Pediatr Cardiol* 2005; **26**: 206–12.

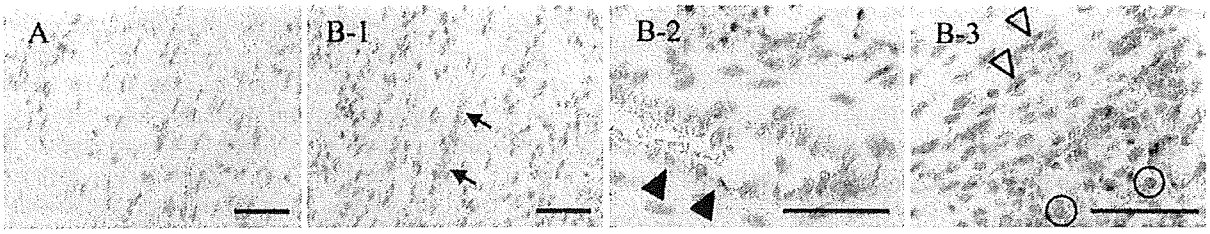

Figure 5. Immunohistochemistry for Lcn2/NGAL in the hearts of a normal rat (A) and an EAM rat on day 17 (B-1–3). Lcn2/NGAL positive cardiomyocytes (arrows), vascular wall cells (arrowhead), spindle-like fibroblastoid cells (white arrow head) and leukocytes (circle) were detected in hearts of EAM rat. Bars=100 μm. EAM, experimental autoimmune myocarditis; Lcn2, lipocalin-2; NGAL, neutrophil gelatinase-B associated lipocalin.

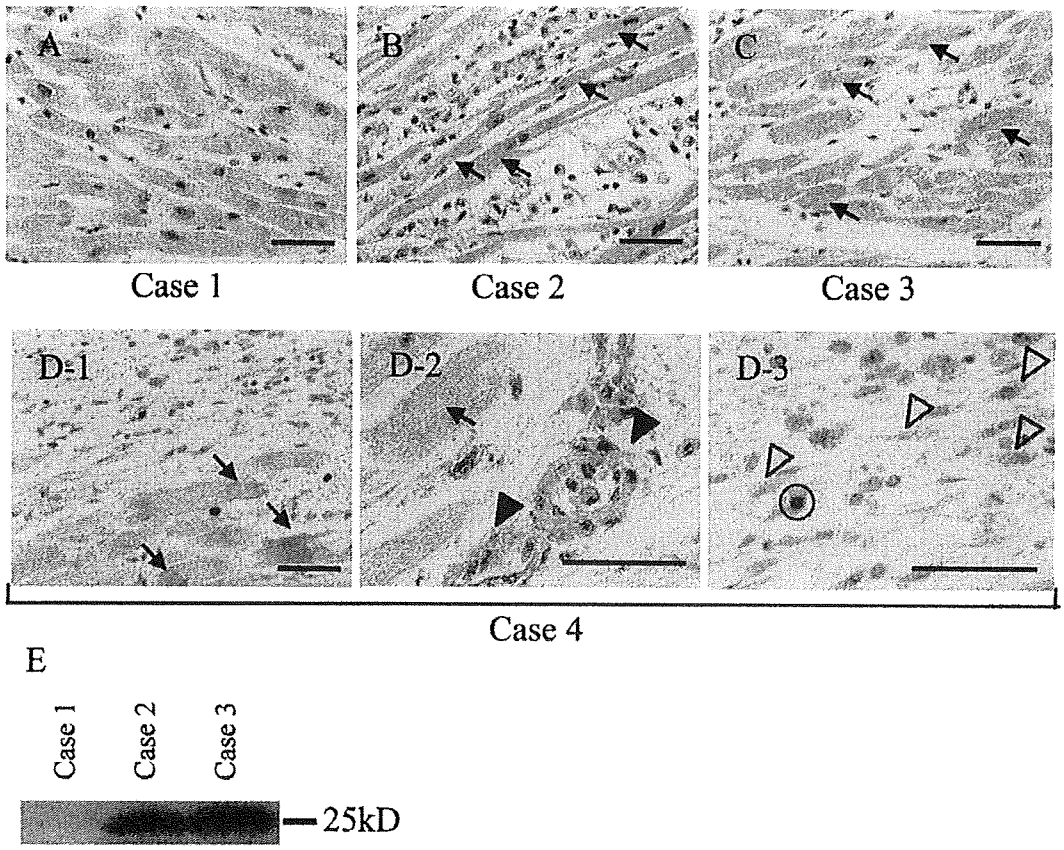

Figure 6. Lcn2/NGAL expression in human hearts. (A–D) Immunohistochemistry for Lcn2/NGAL in hearts of patients with primary pulmonary hypertension (Case 1, A), fulminant myocarditis (Case 2, B), chronic myocarditis (Case 3, C) and fulminant myocarditis (Case 4, D-1, D-2 and D-3). Lcn2/NGAL positive cardiomyocytes (arrows), vascular wall cells (arrowhead), spindle-like fibroblastoid cells (white arrowhead) and leukocytes (circle) were readily detected in hearts of patients with myocarditis. Bars=100 μm. (E) Lcn2/NGAL protein levels by Western blot analysis in the hearts of Cases 1–3. Lcn2, lipocalin-2; NGAL, neutrophil gelatinase-B associated lipocalin.

increased approximately 100-fold on days 12, 15 and 18 compared with normal hearts of 8-week old rats. It then decreased at day 30 and returned to near normal levels at day 60 (Figure 1A). IL-1β expression in the EAM hearts also began to increase at day 9 and increased approximately 700-fold at day 12 and then slowly decreased and returned to near normal levels at day 60 (Figure 1B).

Analysis of Lcn2/NGAL or 24p3R mRNA-Expressing Cells in EAM Hearts

Lcn2/NGAL expressing cells in EAM hearts at day 18 were identified as cardiomyocytes and NCNI cells such as endo-

lopathy have recently been accumulated, the impact of obesity in primary glomerular diseases has rarely been investigated. Only one cohort study demonstrated that excessive body weight was an underestimated predictive factor for the development of arterial hypertension and chronic renal failure in IgA nephropathy [5].

IgA nephropathy is the most common type of primary glomerular disease in the world and remains an important cause of renal failure [6]. IgA nephropathy is histologically characterized by mesangial IgA deposition, and is also known to be frequently associated with glomerular basement membrane (GBM) abnormalities such as thinning, splitting, membranolysis and rupture [7, 8]. On our ultrastructural examination, however, some patients with IgA nephropathy present diffuse GBM thickening. We postulated that obesity might be associated with GBM thickening, which would accelerate disease progression in IgA nephropathy.

The purpose of this study is to investigate the influence of non-diabetic obesity in IgA nephropathy on a variety of clinicopathological parameters including ultrastructural GBM thickness, and to evaluate the outcome of proteinuria after a 1-year follow-up in patients treated with angiotensin-converting enzyme inhibitor (ACE-I) or angiotensin II receptor blocker (ARB).

Patients and Methods

Patients

Among 296 patients who underwent renal biopsy in our institution from October 2000 to January 2004, 108 patients were diagnosed with IgA nephropathy. Among these IgA nephropathy patients, 74 patients with adequate glomerular tissue for electron microscopical examination were included in this study. Patients with diabetes mellitus (fasting blood glucose level ≥126 mg/dl, random blood glucose level ≥200 mg/dl, or currently on antidiabetes medications) or autoimmune diseases were excluded. The study protocol was approved by the Ethics Committee of Kitano Hospital.

Patients were divided into two groups according to body mass index (BMI). BMI was calculated as body weight in kilograms divided by height in squared meters. The WHO and NIH define obesity as BMI ≥30 kg/m^2 [9, 10], while the Japan Society for the Study of Obesity defines obesity as BMI ≥25 kg/m^2 [11]. In this study, the obese group (group O) was defined as BMI ≥25 kg/m^2, and the non-obese group (group N) as BMI <25 kg/m^2 according to the Japanese criteria for obesity.

For all patients, we collected the following data at the time of renal biopsy: (1) physiological findings: gender, age, height, body weight, presence of hypertension (systolic blood pressure ≥140 mm Hg, diastolic blood pressure ≥90 mm Hg, or currently on antihypertensive drugs); (2) laboratory findings: 24-hour urinary protein excretion, creatinine clearance adjusted for body surface area, hematuria (red blood cell counts per high-power field in the urine sediment), serum creatinine, blood urea nitrogen, serum albumin, serum immunoglobulin A, total cholesterol; (3) pathological findings: light microscopical examination, immunofluorescence examination of IgA, electron microscopical examination of GBM thickness, and immunohistochemical examination of α-smooth muscle actin (α-SMA). Hemoglobin A1c (HbA1c), plasma renin activity (PRA) and plasma aldosterone were collected from 45 patients (30 patients in group N and 15 patients in group O).

Tissue Preparation

Renal tissues were obtained by percutaneous needle biopsy. For light microscopy, one sample of renal tissue was fixed in buffered 10% formaldehyde and the other in Dubosq-Brazil solution, and embedded in paraffin. Sections (5 μm) were stained with the following reagents: (1) hematoxylin and eosin; (2) periodic acid-Schiff (PAS); (3) periodic acid-methenamine silver (PAM), and (4) immunohistochemical reagent for detection of α-SMA. Extrarenal tissue was taken for immunofluorescence (IgA, IgG, IgM, C3, C4, C1q, fibrinogen) and electron microscopy.

For electron microscopy, small pieces of renal tissue were fixed in 2% glutaraldehyde solution buffer and postfixed in 1% osmic acid. After embedding, ultrathin sections were stained with uranyl acetate and lead citrate. These were observed and photographed with an H-600 electron microscope (Hitachi, Japan).

Morphometric Analysis

Morphometric analysis was performed by a nephrologist in a blinded fashion.

Light Microscopy. By light microscopy, six parameters (global sclerosis, segmental sclerosis, crescents, mesangial cell proliferation, mesangial matrix expansion, tubular atrophy/interstitial fibrosis) were evaluated. The extent of global sclerosis, segmental sclerosis and crescents (cellular and fibrocellular crescents) was expressed as the percentage of affected glomeruli over total glomeruli obtained. Mesangial cell proliferation and mesangial matrix expansion were semiquantitatively graded from 0 to 3: grade 0, absent; grade 1, mild; grade 2, moderate; grade 3, severe. Tubular atrophy/interstitial fibrosis was graded as follows: grade 0, absent; grade 1, 1–24%; grade 2, 25–49%; grade 3, ≥50%.

Immunofluorescence Microscopy. By immunofluorescence microscopy, the intensity of glomerular IgA staining was semiquantitatively graded from 1 to 3: grade 1, mild; grade 2, moderate; grade 3, severe.

Image Analysis. The glomerular area was quantified using PAS-stained sections. Only glomeruli containing visible stalks were used for area measurements. Glomeruli were digitized using a camera attached to a microscope. After digitalization, Bowman's capsule, the glomerular tuft and mesangial matrix were traced and each area was calculated using the National Institutes of Health (NIH) Image program. The volume of mesangial matrix was expressed as the percentage of matrix area over the glomerular tuft area. Glomerular α-SMA expression was also quantified by computer-aided image analysis. The results were expressed as the percentage of α-SMA-positive area over the glomerular tuft area.

GBM Measurements. Thicknesses of lamina rara interna, the sum of lamina densa and lamina rara externa were measured at 10 equally distributed points of cross-section passing through the

Although iron is an essential nutrient in all cells,[25] enhanced oxidative stress because of excessive iron may cause lethal damage to cells.[26] In a recent study we demonstrated that expression of hepcidin, another novel protein involved in iron transport, was increased in cardiomyocytes in myocarditis or acute myocardial infarction.[21] In the presence of massive cardiac injury, proteins that are involved in iron transport may play an important role in iron homeostasis. We speculate that they may act by reducing extracellular iron concentrations in the heart, perhaps through the mechanism of sequestering, storing, and detoxification in the form of ferritin.[27] Thus they may play an important cytoprotective role against extracellular free radical formation by inhibiting an increase in the extracellular iron concentration. It has also been reported that Lcn2/NGAL prevents H_2O_2 toxicity, which is considered to be an inducer of oxidative stress caused by reactive oxygen species generation, thus providing a potential beneficial effect in ameliorating the toxicity induced by oxidative stress conditions.[5] However, further studies are needed to elucidate in full the functions of Lcn2/NGAL in cardiac injury.

Recently several studies have shown that plasma and urine Lcn2/NGAL levels might be useful biomarkers of acute renal failure,[8,9,11,28,29] and it has been suggested that proximal tubules produce Lcn2/NGAL in acute renal failure.[30,31] In our current study we demonstrated that expression of Lcn2/NGAL was greatest in hearts and livers. Although it remains unknown why the livers in EAM rats express Lcn2/NGAL so prominently, we speculate that this may be caused by high plasma IL-1 levels or liver congestion because of heart failure. In any case, if multiple organ failure occurs, high plasma Lcn2/NGAL levels should be carefully evaluated, considering that several organs can express Lcn2/NGAL. Moreover, in the presence of dramatic changes such as occur in myocarditis, plasma Lcn2/NGAL levels should also be evaluated with respect to the stage of disease. Biomarkers that predict preexisting heart disease and the severity of cardiac remodeling are greatly needed.[32-34] The present study suggests that Lcn2/NGAL is strongly expressed and induced by proinflammatory cytokines in hearts with myocarditis and we speculate that it may play a cytoprotective role by transporting iron into cells and thus may be a useful biomarker of inflammatory heart disease, but further studies are needed to evaluate the full potential of Lcn2/NGAL.

Acknowledgments

This study was supported in part by a Ministry of Health, Labor and Welfare in Japan Grant "Research on Regulatory Science of Pharmaceutical and Medical Devices." and by a Grant for scientific research from the Ministry of Education, Culture, Sports, Science and Technology of Japan (no. 20591185).

References

1. Kjeldsen L, Johnsen AH, Sengelov H, Borregaard N. Isolation and primary structure of NGAL, a novel protein associated with human neutrophil gelatinase. *J Biol Chem* 1993; **268:** 10425–10432.
2. Flo TH, Smith KD, Sato S, Rodriguez DJ, Holmes MA, Strong RK, et al. Lipocalin 2 mediates an innate immune response to bacterial infection by sequestrating iron. *Nature* 2004; **432:** 917–921.
3. Devireddy LR, Gazin C, Zhu X, Green MR. A cell-surface receptor for lipocalin 24p3 selectively mediates apoptosis and iron uptake. *Cell* 2005; **123:** 1293–1305.
4. Richardson DR. 24p3 and its receptor: Dawn of a new iron age? *Cell* 2005; **123:** 1175–1177.
5. Roudkenar MH, Halabian R, Ghasemipour Z, Roushandeh AM, Rouhbakhsh M, Nekogoftar M, et al. Neutrophil gelatinase-associated lipocalin acts as a protective factor against H(2)O(2) toxicity. *Arch Med Res* 2008; **39:** 560–566.
6. Cowland JB, Sorensen OE, Sehested M, Borregaard N. Neutrophil gelatinase-associated lipocalin is up-regulated in human epithelial cells by IL-1 beta, but not by TNF-alpha. *J Immunol* 2003; **171:** 6630–6639.
7. Schmidt-Ott KM, Mori K, Li JY, Kalandadze A, Cohen DJ, Devarajan P, et al. Dual action of neutrophil gelatinase-associated lipocalin. *J Am Soc Nephrol* 2007; **18:** 407–413.
8. Mishra J, Dent C, Tarabishi R, Mitsnefes MM, Ma Q, Kelly C, et al. Neutrophil gelatinase-associated lipocalin (NGAL) as a biomarker for acute renal injury after cardiac surgery. *Lancet* 2005; **365:** 1231–1238.
9. Poniatowski B, Malyszko J, Bachorzewska-Gajewska H, Malyszko JS, Dobrzycki S. Serum neutrophil gelatinase-associated lipocalin as a marker of renal function in patients with chronic heart failure and coronary artery disease. *Kidney Blood Press Res* 2009; **32:** 77–80.
10. Hirsch R, Dent C, Pfriem H, Allen J, Beekman RH 3rd, Ma Q, et al. NGAL is an early predictive biomarker of contrast-induced nephropathy in children. *Pediatr Nephrol* 2007; **22:** 2089–2095.
11. Damman K, van Veldhuisen DJ, Navis G, Voors AA, Hillege HL. Urinary neutrophil gelatinase associated lipocalin (NGAL), a marker of tubular damage, is increased in patients with chronic heart failure. *Eur J Heart Fail* 2008; **10:** 997–1000.
12. Aigner F, Maier HT, Schwelberger HG, Wallnofer EA, Amberger A, Obrist P, et al. Lipocalin-2 regulates the inflammatory response during ischemia and reperfusion of the transplanted heart. *Am J Transplant* 2007; **7:** 779–788.
13. Roudkenar MH, Kuwahara Y, Baba T, Roushandeh AM, Ebishima S, Abe S, et al. Oxidative stress induced lipocalin 2 gene expression: Addressing its expression under the harmful conditions. *J Radiat Res (Tokyo)* 2007; **48:** 39–44.
14. Yndestad A, Landro L, Ueland T, Dahl CP, Flo TH, Vinge LE, et al. Increased systemic and myocardial expression of neutrophil gelatinase-associated lipocalin in clinical and experimental heart failure. *Eur Heart J* 2009; **30:** 1229–1236.
15. Watanabe R, Hanawa H, Yoshida T, Ito M, Isoda M, Chang H, et al. Gene expression profiles of cardiomyocytes in rat autoimmune myocarditis by DNA microarray and increase of regenerating gene family. *Transl Res* 2008; **152:** 119–127.
16. Liu H, Hanawa H, Yoshida T, Elnaggar R, Hayashi M, Watanabe R, et al. Effect of hydrodynamics-based gene delivery of plasmid DNA encoding interleukin-1 receptor antagonist-Ig for treatment of rat autoimmune myocarditis: Possible mechanism for lymphocytes and noncardiac cells. *Circulation* 2005; **111:** 1593–1600.
17. Chang H, Hanawa H, Yoshida T, Hayashi M, Liu H, Ding L, et al. Alteration of IL-17 related protein expressions in experimental autoimmune myocarditis and inhibition of IL-17 by IL-10-Ig fusion gene transfer. *Circ J* 2008; **72:** 813–819.
18. Lane JR, Neumann DA, Lafond-Walker A, Herskowitz A, Rose NR. Role of IL-1 and tumor necrosis factor in coxsackie virus-induced autoimmune myocarditis. *J Immunol* 1993; **151:** 1682–1690.
19. Loppnow H, Westphal E, Buchhorn R, Wessel A, Werdan K. Interleukin-1 and related proteins in cardiovascular disease in adults and children. *Shock* 2001; **16:** 3–9.
20. Yoshida T, Hanawa H, Toba K, Watanabe H, Watanabe R, Yoshida K, et al. Expression of immunological molecules by cardiomyocytes and inflammatory and interstitial cells in rat autoimmune myocarditis. *Cardiovasc Res* 2005; **68:** 278–288.
21. Isoda M, Hanawa H, Watanabe R, Yoshida T, Toba K, Yoshida K, et al. Expression of the peptide hormone hepcidin increases in cardiomyocytes under myocarditis and myocardial infarction. *J Nutr Biochem* 2009 [E-pub ahead of print].
22. Kodama M, Matsumoto Y, Fujiwara M, Masani F, Izumi T, Shibata A. A novel experimental model of giant cell myocarditis induced in rats by immunization with cardiac myosin fraction. *Clin Immunol Immunopathol* 1990; **57:** 250–262.
23. Walters FP, Kennedy FG, Jones DP. Oxidation of myoglobin in isolated adult rat cardiac myocytes by 15-hydroperoxy-5,8,11,13-eicosatetraenoic acid. *FEBS Lett* 1983; **163:** 292–296.
24. Baron CP, Andersen HJ. Myoglobin-induced lipid oxidation: A review. *J Agric Food Chem* 2002; **50:** 3887–3897.
25. Aisen P, Enns C, Wessling-Resnick M. Chemistry and biology of eukaryotic iron metabolism. *Int J Biochem Cell Biol* 2001; **33:** 940–959.
26. Halliwell B, Gutteridge JM. Biologically relevant metal ion-dependent hydroxyl radical generation: An update. *FEBS Lett* 1992; **307:** 108–112.
27. Balla G, Jacob HS, Balla J, Rosenberg M, Nath K, Apple F, et al. Ferritin: A cytoprotective antioxidant strategem of endothelium.

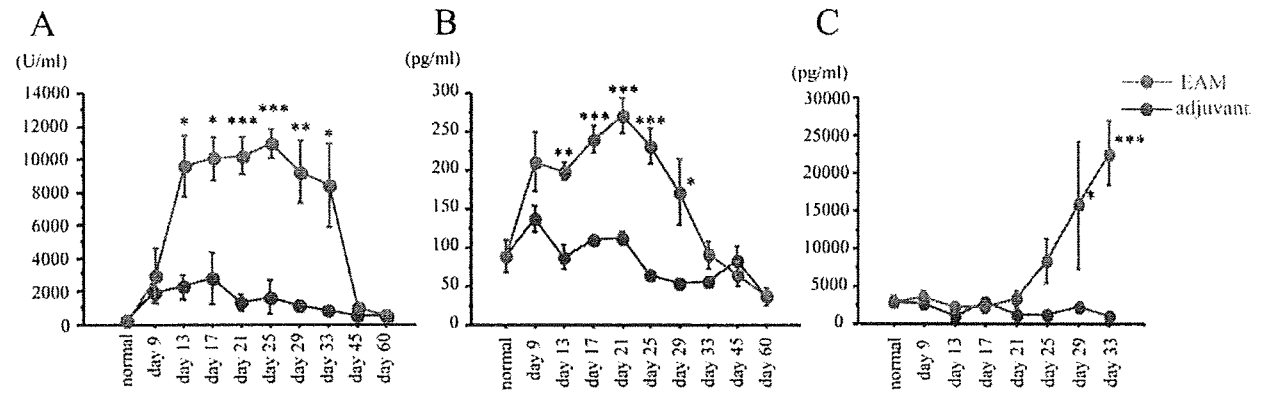

Figure 3. Plasma levels of Lcn2/NGAL (A), IL-1β (B) and BNP (C) measured by ELISA in normal, adjuvant control, and EAM rats (n=4 for each). Statistical assessment was performed by 1-way ANOVA and Bonferroni's multiple comparison test. Differences were considered significant at P<0.05. ***P<0.001 vs normal rat; **P<0.01 vs normal rat; *P<0.05 vs normal rat. EAM, experimental autoimmune myocarditis; IL-1, interleukin-1; Lcn2, lipocalin-2; NGAL, neutrophil gelatinase-B associated lipocalin; BNP, B-type natriuretic peptide.

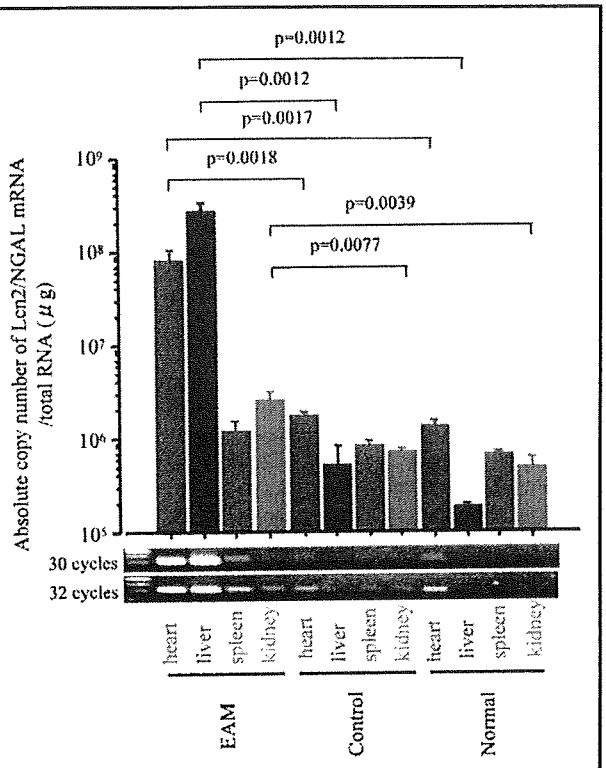

Figure 4. Gene expression of Lcn2/NGAL mRNA in organs of EAM and control rats killed on day 13, and in normal rats (n=4 in each group). Portions of their hearts, livers, spleens, and kidneys were collected. PCR bands after 30 and 32 cycles were visualized by ethidium bromide. Statistical assessment was performed by one-way ANOVA and Bonferroni's multiple comparison test. Differences were considered significant at P<0.05. EAM, experimental autoimmune myocarditis; IL-1, interleukin-1; Lcn2, lipocalin-2; NGAL, neutrophil gelatinase-B associated lipocalin; PCR, polymerase chain reaction.

horseradish peroxidase-labeled anti-rat antibody (Santa Cruz Biotechnology, Santa Cruz, CA, USA) in TBS with 0.05% Triton X-100. The membranes were exposed to a chemiluminescent reagent (GE Healthcare, Buckingham, UK) and autoradiographed for 10s.

Heart Samples From Heart Failure Patients

Four autopsied human hearts from individuals who had died of cardiac failure (Case 1: 20-year-old woman diagnosed as having primary pulmonary hypertension; Case 2: 66-year-old man with fulminant myocarditis diagnosed at autopsy; Case 3: 64-year-old man diagnosed at autopsy as having chronic myocarditis; Case 4: 62-year-old man with fulminant myocarditis diagnosed at autopsy) were evaluated by immunohistochemistry. Samples collected from hearts of 26 previously reported patients[21] (19 patients without myocarditis, 7 patients with myocarditis) were examined for the expression of Lcn2/NGAL by real-time RT-PCR analysis. Lcn2/NGAL in the hearts of Cases 1, 2 and 3 were analyzed by Western blot analysis.

The local ethics committee approved this study, and families of all patients signed informed consent in relation to diagnosis by histological examination, including gene expression analyses.

Statistical Analysis

Statistical assessment was performed by 1-way ANOVA and Bonferroni's multiple comparison test or the Mann-Whitney U test. Differences were considered significant at P<0.05. Data obtained from quantitative RT-PCR were expressed as mean±SEM.

Results

Time Course of Lcn2/NGAL and IL-1β Expression in EAM Hearts

A previous study reported that inflammatory cells begin to infiltrate the heart of EAM rats at approximately day 12, peak at approximately days 14–21, and disappear after day 21, followed by progressive fibrosis.[22] In our study, Lcn2/NGAL expression in EAM hearts started to rise at day 9 and

Original Paper

nephron Clinical Practice

Nephron Clin Pract 2009;112:c71–c78
DOI: 10.1159/000213084

Received: July 1, 2008
Accepted: November 13, 2008
Published online: April 18, 2009

Impact of Obesity on IgA Nephropathy: Comparative Ultrastructural Study between Obese and Non-Obese Patients

Mari Tanaka[a] Sachiko Yamada[a] Yukako Iwasaki[a] Takeshi Sugishita[a] Satomi Yonemoto[a] Tatsuo Tsukamoto[a] Satoshi Fukui[b] Kosho Takasu[b] Eri Muso[a]

Departments of [a]Nephrology and Dialysis and [b]Pathology, Kitano Hospital, Tazuke Kofukai Medical Research Institute, Osaka, Japan

Key Words

Body mass index · Glomerular basement membrane · Glomerular hypertrophy · IgA nephropathy · Proteinuria · Obesity · Overweight

Abstract

Background: The pathological role of obesity in the progression of glomerular lesions has rarely been studied in primary glomerular diseases. The purpose of this study is to investigate the influence of non-diabetic obesity on clinicopathological findings in IgA nephropathy. ***Methods:*** 74 patients with biopsy-proven IgA nephropathy were retrospectively divided into two groups according to the criteria for obesity in Japan: non-obese group (group N: n = 50) with BMI <25 kg/m^2, and obese group (group O: n = 24) with BMI ≥25 kg/m^2. Clinical and pathological data at the time of renal biopsy were analyzed. Moreover, the outcome of proteinuria in patients treated with angiotensin-converting enzyme inhibitors (ACE-I) or angiotensin II receptor blockers (ARB) was evaluated in different groups after a 1-year follow-up. ***Results:*** Urinary protein excretion was significantly greater in the obese group compared to normal-weight patients ($p < 0.05$). There was no significant difference in the prevalence of hypertension and hyperlipidemia. By light microscopy, the obese group showed significantly larger glomerular size ($p < 0.0001$). On the other hand, the severity of mesangial matrix expansion and crescent formation revealed no difference between the two groups. By electron microscopy, glomerular basement membrane (GBM) thickness was significantly increased in obese patients ($p < 0.001$). Among 61 patients who were followed up for 1 year in our institute, 15 patients were treated with ACE-I or ARB without steroids. ACE-I or ARB treatment without steroids tended to reduce proteinuria in the obese patients, but this change did not achieve statistical significance. ***Conclusions:*** In IgA nephropathy, obesity induces not only glomerular enlargement but also ultrastructural modification of GBM, which would contribute to increase proteinuria.

Introduction

The prevalence of obesity has markedly increased in the past few decades because of changing dietary habits and lifestyle [1]; therefore, more attention has been paid to the renal effects of obesity as obesity-related glomerulopathy. Obesity-related glomerulopathy is characterized histologically by glomerulomegaly and focal segmental glomerulosclerosis [2, 3], and clinically by poor renal outcome [3, 4]. Although data on obesity-related glomeru-

KARGER

Fax +41 61 306 12 34
E-Mail karger@karger.ch
www.karger.com

1660–2110/09/1122–0071$26.00/0

Accessible online at:
www.karger.com/nec

Eri Muso
Department of Nephrology and Dialysis, Kitano Hospital
Tazuke Kofukai Medical Research Institute
2-4-20 Ohgimachi, Kita-ku, Osaka 530-8480 (Japan)
Tel. +81 6 6312 1221, Fax +81 6 6312 8867, E-Mail muso@kitano-hp.or.jp

Table 4. Determinants of GBM thickness (univariate and multivariate linear regression analysis; n = 74)

Independent variables	Univariate		Multivariate[1]	
	correlation (r)	p value	standardized coefficient (β)	p value
Mesangial matrix expansion	0.353	0.002	0.074	0.573
BMI	0.312	0.007	0.270	0.056
Urinary protein excretion	0.196	0.094	0.055	0.690
Intensity of glomerular IgA	0.196	0.131	0.252	0.067
Mesangial cell proliferation	0.115	0.328	−0.076	0.568
Crescents	0.095	0.422	−0.205	0.149

GBM = Glomerular basement membrane; BMI = body mass index.
[1] $R^2 = 0.17$.

only BMI was a significant predictor of the GBM thickening. On the other hand, in multivariate linear regression analysis using GBM thickness as a continuous variable, BMI tended to be associated with GBM thickness, but this did not reach statistical significance (table 4). In both multivariate analyses, the other variables were not associated with GBM thickness.

Change in Proteinuria during a One-Year Follow-Up in Patients Treated with ACE-I or ARB

61 patients (46 patients in group N and 15 patients in group O) were followed up for 1 year in our institute. We started steroid treatment when cellular and fibrocellular crescents were more than 10% of all glomeruli. Patients with current hypertension or with persistent proteinuria >0.2 g/24 h were treated with ACE-I or ARB. 15 patients (6 patients in group N and 9 patients in group O) were treated with ACE-I or ARB without steroid. Patients treated with ACE-I or ARB in group N showed no significant decrease in proteinuria during the follow-up period (557.5 ± 241.3 to 419.3 ± 108.9 mg/g Cre, $p = 0.253$). In group O, 7 of 9 patients who received ACE-I or ARB treatment without steroid showed ameliorated proteinuria, but the difference did not achieve statistical significance (815.6 ± 474.9 to 259.5 ± 74.9 mg/g Cre, $p = 0.109$). The BMI of these 7 patients significantly decreased during a 1-year follow-up (26.5 ± 0.7 to 25.2 ± 0.7 kg/m^2, $p < 0.05$), whereas the BMI of 2 patients whose proteinuria did not ameliorate was unchanged. Reduction in BMI, however, did not correlate with decrease in proteinuria among these patients (n = 9, rs = 0.07805, p = 0.427).

Discussion

In view of the high prevalence of obesity and obesity-related disorders, more attention is recently being focused on the relationship between obesity and renal function. Obesity is associated with specific pathological features such as glomerulomegaly and focal segmental glomerulosclerosis, termed obesity-related glomerulopathy [2–4]. Although data on obesity-related glomerulopathy have recently been accumulated, the influence of obesity in primary glomerular diseases has rarely been investigated. This is the first study which investigates the impact of non-diabetic obesity on pathological glomerular lesions in IgA nephropathy by quantitative analysis.

The present study demonstrated that non-diabetic obese patients in IgA nephropathy showed significant increased proteinuria, accompanied by GBM thickening and glomerulomegaly. On the other hand, histological markers of disease activity such as the extent of mesangial matrix expansion, mesangial cell proliferation, crescent formation, glomerular α-SMA expression and glomerular IgA deposition were not different between non-obese and obese patients. Cell numbers per glomeruli by quantitative analysis were also similar between the two groups, but cell numbers divided by tuft area were rather less in obese patients than those in non-obese patients. In this study, the ratio of men to women was higher in the obese group than in the non-obese group. Therefore, we performed a comparison between non-obese and obese groups among only male patients in order to exclude gender differences, and the same results were obtained. These results indicate that the glomerular structural changes we observed, GBM thickening and glomerulomegaly, might at least partly contribute to increased proteinuria

center of a glomerular capillary on an electron micrograph at magnification ×8,000. Tangentially sectioned GBM was excluded from the measurement. The average of the 10 measurements per patient was calculated.

Statistical Analysis

Data were reported as the mean ± SD. Unpaired Student's t test was used to compare the mean between the two groups. The comparison of proportions was assessed by χ^2 test. Spearman correlation analysis was performed to examine the relationship between GBM thickness and urinary protein excretion. Multivariate regression analysis was performed to assess determinants of GBM thickening. Statistical significance was considered as $p < 0.05$.

Results

Comparison of Clinical Parameters at the Time of Renal Biopsy

There were 50 patients in group N (17 men and 33 women) and 24 patients in group O (18 men and 6 women). Clinical parameters at the time of renal biopsy are listed in table 1. The two groups were similar in the distribution of age, hypertension and antihypertensive drugs, but the ratio of men to women was significantly higher in group O.

Urinary protein excretion and serum creatinine were significantly greater in group O than group N. Other laboratory parameters such as creatinine clearance, total cholesterol, HbA1c, PRA and aldosterone showed no statistical difference between the two groups.

Serum creatinine is well recognized to be dependent on muscle mass and therefore on gender. As the ratio of men to women was higher in group O, a comparison of only male patients between the two groups was performed. The number of male patients was almost equal between the two groups (17 patients in group N, 18 patients in group O). As shown in table 1, this comparison showed no significant difference in all parameters including serum creatinine, except urinary protein excretion. Urinary protein excretion was still significantly greater in group O male patients than in group N male patients.

Comparison of Findings by Light and Immunofluorescence Microscopy and Image Analysis

Findings by light and immunofluorescence microscopy and image analysis are shown in table 2. By light microscopy, there were no significant differences between the two groups in all parameters such as glomerulosclerosis, crescent formation, semiquantitative severity of

Table 1. Clinical parameters at the time of renal biopsy[1]

	Group N	Group O	p value
Patients	50	24	
Male/female	17/33	18/6	<0.01
Age, years	38.5 ± 15.8	42.3 ± 15.6	NS
	43.8 ± 16.3	44.8 ± 14.9	NS
Height, cm	160.8 ± 7.7	166.8 ± 8.2	<0.01
	167.7 ± 7.5	170.4 ± 5.7	NS
Body weight, kg	55.1 ± 9.1	78.2 ± 11.9	<0.0001
	63.9 ± 6.4	82.4 ± 10.1	<0.0001
BMI	21.2 ± 2.5	28.0 ± 2.0	<0.0001
	22.7 ± 1.8	28.4 ± 3.0	<0.0001
Hypertension, %	14 (28.0)	9 (37.5)	NS
	6 (35.3)	8 (44.4)	NS
Proteinuria, g/24 h	0.43 ± 0.50	0.74 ± 0.83	<0.05
	0.43 ± 0.46	0.83 ± 0.86	<0.05
Ccr, ml/min/1.73 m^2	112.8 ± 28.3	106.0 ± 37.1	NS
	105.5 ± 38.4	97.7 ± 38.2	NS
Hematuria[2]	2.5 ± 1.4	2.6 ± 1.4	NS
	2.4 ± 1.5	2.3 ± 1.4	NS
Serum creatinine, mg/dl	0.73 ± 0.23	0.97 ± 0.44	<0.001
	0.98 ± 0.22	1.10 ± 0.44	NS
BUN, mg/dl	14.4 ± 4.9	14.4 ± 4.8	NS
	17.4 ± 6.0	15.6 ± 4.9	NS
Serum albumin, g/dl	4.16 ± 0.42	4.16 ± 0.39	NS
	4.14 ± 0.47	4.19 ± 0.33	NS
Serum IgA, mg/dl	331 ± 157	347 ± 126	NS
	327 ± 140	362 ± 122	NS
Serum cholesterol, mg/dl	199 ± 38	193 ± 31	NS
	201 ± 40	197 ± 33	NS
HbA1c, %	4.6 ± 0.3 (n = 30)	4.9 ± 0.6 (n = 15)	NS
	4.5 ± 0.4 (n = 11)	4.9 ± 0.4 (n = 10)	NS
PRA, ng/ml/h	1.9 ± 1.4 (n = 30)	1.8 ± 1.4 (n = 15)	NS
	2.3 ± 1.9 (n = 10)	2.1 ± 1.5 (n = 11)	NS
Aldosterone, pg/ml	122 ± 115 (n = 30)	111 ± 57 (n = 15)	NS
	103 ± 46 (n = 10)	111 ± 51 (n = 11)	NS

BMI = Body mass index; ACE-I = angiotensin-converting enzyme inhibitor; ARB = angiotensin II receptor blocker; Ca blocker = calcium channel blocker; Ccr = creatinine clearance adjusted for body surface area; BUN = blood urea nitrogen; HbA1c = hemoglobin A1c; PRA = plasma renin activity; NS = not significant.

[1] Upper values: comparison of all patients; lower values: comparison of male patients.

[2] Grade 0: 0–4, grade 1: 5–9, grade 2: 10–29, grade 3: 30–99, grade 4 ≥100 red blood cell counts/high-power field.

J Biol Chem 1992; **267:** 18148–18153.
28. Bolignano D, Donato V, Coppolino G, Campo S, Buemi A, Lacquaniti A, et al. Neutrophil gelatinase-associated lipocalin (NGAL) as a marker of kidney damage. *Am J Kidney Dis* 2008; **52:** 595–605.
29. Bolignano D, Basile G, Parisi P, Coppolino G, Nicocia G, Buemi M. Increased plasma neutrophil gelatinase-associated lipocalin levels predict mortality in elderly patients with chronic heart failure. *Rejuvenation Res* 2009; **12:** 7–14.
30. Schmidt-Ott KM, Mori K, Kalandadze A, Li JY, Paragas N, Nicholas T, et al. Neutrophil gelatinase-associated lipocalin-mediated iron traffic in kidney epithelia. *Curr Opin Nephrol Hypertens* 2006; **15:** 442–449.
31. Mishra J, Ma Q, Prada A, Mitsnefes M, Zahedi K, Yang J, et al. Identification of neutrophil gelatinase-associated lipocalin as a novel early urinary biomarker for ischemic renal injury. *J Am Soc Nephrol* 2003; **14:** 2534–2543.
32. Saiki A, Iwase M, Takeichi Y, Umeda H, Ishiki R, Inagaki H, et al. Diversity of the elevation of serum cardiac troponin I levels in patients during their first visit to the emergency room. *Circ J* 2007; **71:** 1458–1462.
33. Terasaki F, Okamoto H, Onishi K, Sato A, Shimomura H, Tsukada B, et al. Higher serum tenascin-C levels reflect the severity of heart failure, left ventricular dysfunction and remodeling in patients with dilated cardiomyopathy. *Circ J* 2007; **71:** 327–330.
34. Okamoto H. Can adiponectin be a novel metabolic biomarker for heart failure? *Circ J* 2009; **73:** 1012–1013.

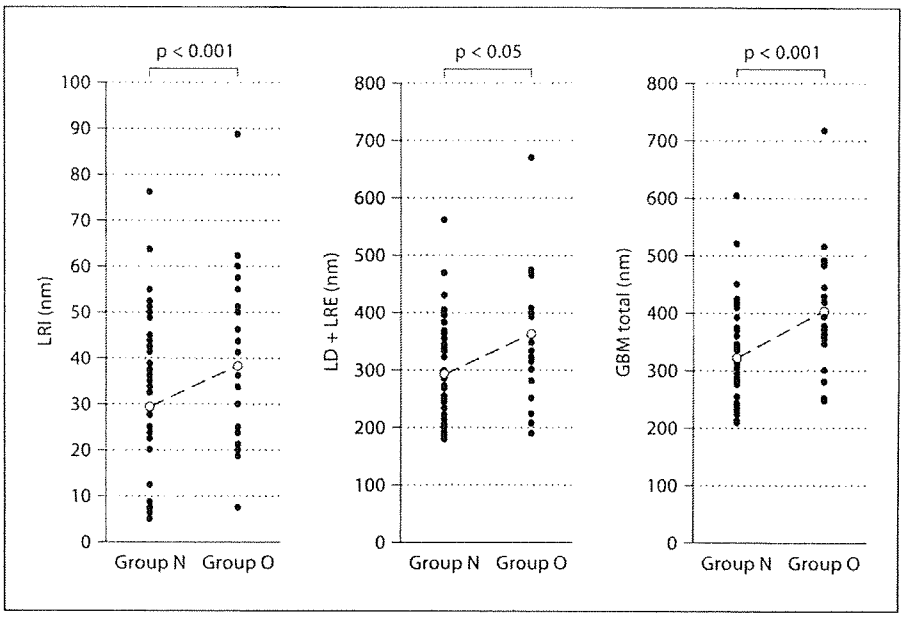

Fig. 1. Comparison of GBM thickness between non-obese and obese groups. GBM thickness is significantly increased in the obese group. LRI = Lamina rara interna; LD = lamina densa; LRE = lamina rara externa; GBM = glomerular basement membrane.

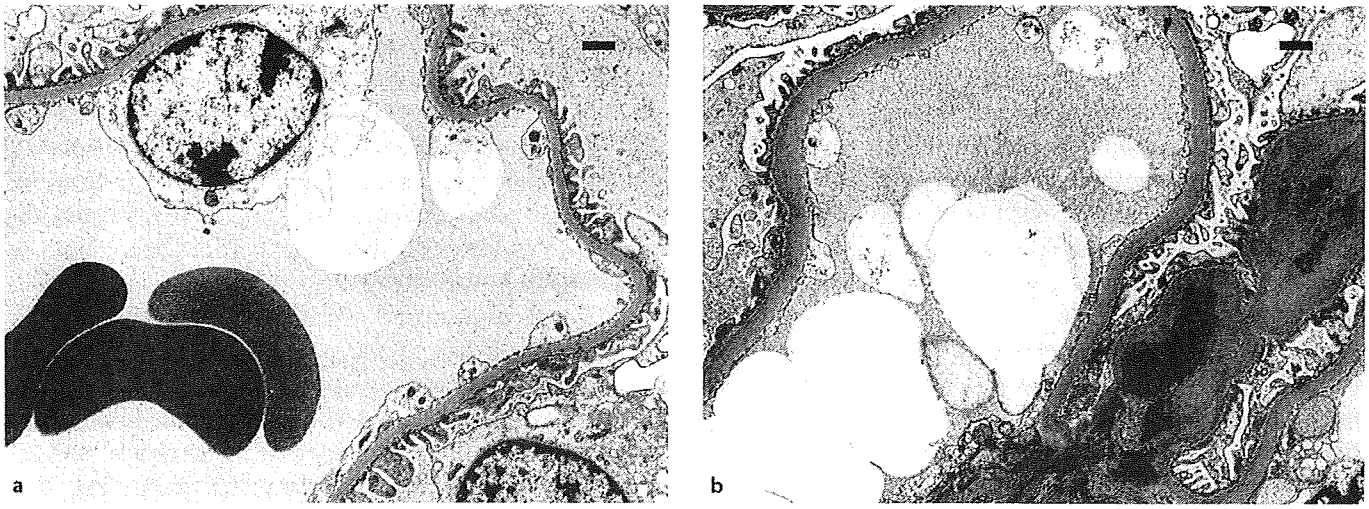

Fig. 2. Representative electron micrographs of glomerular basement membrane (scale bar = 1 μm). An obese patient (**b**) shows diffuse GBM thickening compared with a non-obese patient (**a**).

Determinants of GBM Thickening

In order to assess determinants of GBM thickening, multivariate regression analysis was performed. Variables with $p < 0.10$ in univariate analysis and histological markers of IgA nephropathy activity were entered into multivariate analysis. The following variables were included: mesangial matrix expansion, BMI, urinary protein excretion, the intensity of glomerular IgA staining, mesangial cell proliferation and crescents. Total glomerular area and serum creatinine were excluded because of the close correlation with BMI. Caramori et al. [12] reported that GBM thickness derived from 83 normal living kidney donors was 329 ± 45 nm. Based on these data, we defined GBM thickening as ≥420 nm (mean ± 2 SD) and performed multivariate logistic regression analysis using binarized GBM thickness. As shown in table 3,

serum IgA with increased molecular size and abnormal glycosylation [1, 2]. It is recognized that approximately 30% of patients with this disease will progress to end-stage renal failure within 20 years [3]. It is known that macroscopic hematuria in upper respiratory infections in IgA nephropathy are often found, whereas urinary tract infections and gastroenteritis are less commonly observed [4]. In this context, toll-like receptors (TLRs), NOD-like receptors, and RIG-like receptors have been recently recognized as sensors that play roles in innate immune responses against microbial pathogens [5]. Lipopolysaccharide (LPS) is known to induce proinflammatory gene expression through TLR4 and hypercoagulable state, resulting in the expression of tissue factor, an initiator of the extrinsic pathway [6, 7]. Recently, accumulating reports revealed the significance of TLRs in glomerulonephritis. Circulating microbial pathogen-associated components can stimulate immune and nonimmune cells in the kidney, and may exacerbate glomerulonephritis through activation of TLRs [8]. Glomerular mesangial cells express TLR1–4 and TLR6 [9], and promote production of CXC chemokines upon TLR4 activation [10]. Furthermore, CpG-DNA (ligand to TLR9) is shown to have a unique potential to trigger the onset of lupus nephritis via nucleic acid-specific TLR [11].

Mice of ddY, as a spontaneous murine model of IgA nephropathy maintained as a closed colony, were previously used [12]. Recently, a high IgA (HIGA) ddY strain was established as an inbred strain by selective mating of ddY mice with high serum IgA [13, 14]. HIGA mice display characteristics of IgA nephropathy including high serum IgA, polymeric IgA dominance, and mesangioproliferative glomerulonephritis (MsPGN) with IgA deposition [14]. More recently, we have shown by quantitative trait loci analysis that a genetic linkage exists between the hinge region and polymeric IgA dominancy [15], that glomerular IgA deposition is mainly regulated at chromosome 15, and that hyperserum IgA levels synergistically but weakly affect glomerular IgA deposition [16].

A pathogenic role for locally accelerated coagulation accompanying fibrin deposition was reported in various types of active MsPGN including IgA nephropathy and Henoch-Schönlein purpura nephritis [17]. Glomerular expression of tissue factor, the principle initiator of the extrinsic coagulation pathway, is known to be upregulated in human and rabbit crescentic glomerulonephritis [18, 19]. Tissue factor activates factor X to Xa which converts prothrombin to thrombin in concert with the membrane-bound cofactor factor V [20, 21]. In a previous study, we showed that coagulation factor V was colocalized with fibrin in the mesangial area in an active type of IgA nephropathy with mesangial cell proliferation [22]. Furthermore, Monno et al. [23] have shown that factor Xa directly promotes mesangial cell proliferation in vitro. Recently, we have shown that factor Xa induces cellular proliferation through the activation of extracellular regulated kinase 1/2 and p44/42 MAP kinase via protease-activated receptor 2 (PAR2) in cultured human mesangial cells and in rat Thy-1 nephritis, and that DX-9065a, a small synthetic factor Xa inhibitor, suppresses cellular proliferation in vitro and in vivo [24, 25].

It has been reported that fibrinogen plays the role of a potential endogenous TLR4 ligand, and induces chemokine production in podocytes [26]. On the other hand, splenic TLR9 expression was upregulated in 60-week-old ddY mice with severe glomerulonephritis, whereas TLR2 and TLR4 expression did not show any differences among mild and severe groups [27]. Therefore, in the present study, we intended to clarify the roles of coagulation pathway and factor Xa in the proinflammatory process of MsPGN using a mimicking human IgA nephropathy model, HIGA, and young 12-week-old HIGA mice were injected with LPS and continuously administered a factor Xa inhibitor danaparoid. Our results demonstrate important roles for the coagulation system and factor Xa in the aggravation of MsPGN, triggered by LPS as a microbial pathogen.

Materials and Methods

Animals

Twelve-week-old female HIGA and BALB/c mice were obtained from Japan SLC (Shizuoka, Japan). Mice were housed under specific pathogen-free conditions at the animal facilities of the University of Shizuoka. All animal experiments were performed in accordance with institutional guidelines, and the review board of the University of Shizuoka granted ethical permission for this study. Danaparoid was kindly provided by Nippon Organon K.K. (Osaka, Japan).

Experimental Design

HIGA mice at the age of 12 weeks old were intraperitoneally injected with LPS (5 mg/kg body weight; List Biological Laboratories, Campbell, Calif., USA) twice at an interval of 3 days, and kidney specimens were collected 7 days after the second LPS injection (fig. 1). BALB/c mice were chosen as controls according to the previous studies [13, 14]. BALB/c and HIGA mice were each divided into two experimental groups (n = 6): saline-injected (basal) BALB/c, LPS-injected BALB/c, saline-injected (basal) HIGA, and LPS-injected HIGA mice. In an intervention experiment to clarify the role of factor Xa in MsPGN, the factor Xa-targeted anticoagulant danaparoid was injected intraperitoneally after the first LPS injection once daily for 7 days (LPS + danapa-

in non-diabetic obese IgA nephropathy patients, independent of active mesangial lesions.

To our knowledge, only one study investigated the role of increased BMI in IgA nephropathy. Bonnet et al. [5] have reported that obesity (BMI $\geq$25 kg/m^2) was significantly correlated with increased proteinuria in IgA nephropathy, and that BMI was an independent risk factor predictive of the ultimate development of chronic renal failure. By their semiquantitative pathological examination, vascular, tubular and interstitial indices were significantly greater in obese patients, but the glomerular index showed no difference between non-obese and obese patients. Their glomerular index consisted of only three elementary lesions: mesangial cell proliferation, mesangial sclerosis and glomerular sclerosis. In our study, there were no significant differences in tubular damage, interstitial lesions, and three elementary glomerular lesions between non-obese and obese patients. Although the precise reason for these differences is unclear, it may reflect the presence of other metabolic abnormalities in addition to obesity. In contrast to our study, their study showed a significantly high proportion of hypertension or hyperlipidemia in the obese group, which are known to be independent exacerbating factors of tubular and interstitial damage. Of note, our findings indicated that obesity could independently increase proteinuria without these metabolic abnormalities.

The WHO and NIH define overweight as BMI 25–29.9 and obesity as $\geq$30 kg/m^2 [9, 10]. On the other hand, in Japan, the Japan Society for the Study of Obesity defined obesity as BMI $\geq$25 kg/m^2 for the reason that it is not practical to apply Western criteria to Japanese without any modification [11]. This is because the percentage of the population with BMI $\geq$30 kg/m^2 is no more than 2–3% in Japanese and obesity-related diseases increase for BMI $\geq$25 kg/m^2. In the present study, we used a cut-off point for BMI of 25 kg/m^2 according to the Japanese criteria for obesity. There were no severely obese patients with BMI $\geq$35 kg/m^2, and all patients in the obese group had BMI of 25–34.9 kg/m^2. Patients with BMI $\geq$25 kg/m^2 showed significantly glomerulomegaly and GBM thickening but no differences in other glomerular lesions. A recent study by Rea et al. [13], which used a cut-off point for BMI $\geq$30 kg/m^2, also reported that obese living kidney donors showed a larger glomerular area but no differences in other glomerular scores for mesangial matrix expansion, segmental sclerosis and global sclerosis. In another study by Serra et al. [14], obese patients with BMI $\geq$40 kg/m^2 showed mesangial matrix expansion, mesangial cell proliferation and podocyte hypertrophy in addition to glomerulomegaly. These recent studies did not examine the GBM thickness. The cut-off point of BMI for obesity might make the differences in mesangial matrix expansion and mesangial cell proliferation between our study and Serra's study. Importantly, we would emphasize that even patients who are overweight or mild obesity by the WHO definition have already developed significant glomerular structural changes and subsequent increased proteinuria. This finding suggests that early detection and treatment of overweight or obesity should be an important target in the therapeutic approach of IgA nephropathy. Although other markers of obesity, especially waist-to-hip ratio, have recently been proposed as stronger indicators of cardiovascular diseases than BMI [15], we did not evaluate such markers in this study. Further studies will be required to determine whether these markers may be more reliable measures than BMI in renal diseases.

GBM thickening is one of the characteristic features in diabetic nephropathy [16]. Few studies, however, have focused on the relationship between non-diabetic obesity and GBM thickness. Although Henegar et al. [17] reported that obese dogs showed GBM thickening, this finding was not quantitative. We showed significant GBM thickening in non-diabetic obesity by quantitative analysis and a positive correlation between GBM thickening and proteinuria. One important question arisen from our study is whether GBM thickening in obese IgA nephropathy patients is due to obesity itself or due to IgA nephropathy activity accelerated by obesity. Obesity is well known to be associated with inflammation [18], and we could not rule out the possibility that obesity would accelerate glomerular inflammation. However, we think that obesity would induce GBM thickening by itself rather than by accelerating IgA nephropathy activity at least in the stage of mild obesity. This is because the histological markers of IgA nephropathy activity, such as the extent of glomerular crescents, mesangial matrix expansion, α-SMA-positive area in glomeruli, and the intensity of glomerular IgA deposition, showed no statistical difference between obese and non-obese groups. There were no differences in cell numbers per glomeruli and semiquantitative score of mesangial cell proliferation between the two groups. In addition, cell numbers divided by tuft area were rather less in the obese group than those in the non-obese group. Furthermore, multivariate logistic regression analysis to assess determinants of GBM thickening demonstrated that BMI was the only predictor of the GBM thickening. Histological markers of IgA nephropathy activity tested in multivariate analysis were not asso-

Table 2. Findings by light and immunofluorescence microscopy and image analysis[1]

	Group N	Group O	p value
Light microscopy			
Glomerular findings			
Global sclerosis, %	10.9 ± 10.8	15.8 ± 13.1	NS
	12.6 ± 12.0	16.3 ± 13.2	NS
Segmental sclerosis, %	9.8 ± 10.5	8.3 ± 9.3	NS
	9.7 ± 11.0	8.8 ± 10.5	NS
Crescents, %	6.9 ± 8.9	7.7 ± 18.9	NS
	6.9 ± 9.7	9.3 ± 21.6	NS
Mesangial cell proliferation[2]	1.0 ± 0.5	1.0 ± 0.4	NS
	0.9 ± 0.5	1.1 ± 0.4	NS
Mesangial matrix expansion[2]	1.2 ± 0.5	1.1 ± 0.4	NS
	1.2 ± 0.4	1.1 ± 0.4	NS
Tubulointerstitial findings			
Tubular atrophy/fibrosis[3]	1.0 ± 0.4	1.0 ± 0.2	NS
	1.0 ± 0.6	0.9 ± 0.2	NS
Immunofluorescence microscopy			
Glomerular IgA deposition[4]	2.4 ± 0.8	2.5 ± 0.8	NS
	2.6 ± 0.8	2.5 ± 0.8	NS
Image analysis			
Cell numbers per glomeruli, counts	90.6 ± 29.8	94.9 ± 24.3	NS
	90.4 ± 24.9	97.8 ± 24.3	NS
Cell numbers per tuft area, $\times 10^3$ counts/μm^2	5.9 ± 1.3	5.4 ± 1.3	<0.01
	5.6 ± 1.5	5.2 ± 1.3	<0.05
Mesangial matrix area per tuft area, %	20.6 ± 4.7	21.8 ± 13.2	NS
	20.1 ± 4.4	22.8 ± 15.2	NS
Total glomerular area, $\times 10^3$ μm^2	21.2 ± 5.0	26.8 ± 6.0	<0.0001
	22.6 ± 4.8	28.2 ± 5.9	<0.01
Tuft area, $\times 10^3$ μm^2	16.0 ± 5.6	19.0 ± 6.6	<0.0001
	16.9 ± 5.5	20.2 ± 7.1	<0.01
α-SMA-positive area per tuft area, %	5.7 ± 3.8	5.1 ± 3.1	NS
	5.2 ± 2.8	4.1 ± 2.3	NS

α-SMA = α-Smooth muscle actin; NS = not significant.

[1] Upper values: comparison of all patients, lower values: comparison of male patients.

[2] Grade 0: absent, grade 1: mild, grade 2: moderate, grade 3: severe.

[3] Grade 0: absent, grade 1: 1–24%, grade 2: 25–49%, grade 3: ≥50%.

[4] Grade 1: mild, grade 2: moderate, grade 3: severe.

Table 3. Determinants of GBM thickening[1] (multivariate logistic regression analysis; n = 74)

Independent variables	OR	95% CI	p value
Mesangial matrix expansion	0.793	0.623–1.009	0.059
BMI	0.743	0.571–0.967	0.027
Urinary protein excretion	2.344	0.476–11.548	0.295
Intensity of glomerular IgA	0.312	0.069–1.411	0.130
Mesangial cell proliferation	1.042	0.986–1.102	0.147
Crescents	1.073	0.901–1.278	0.429

GBM = Glomerular basement membrane; OR = odds ratio; CI = confidence interval; BMI = body mass index.

[1] GBM thickening was defined as ≥420 nm.

mesangial cell proliferation, mesangial matrix expansion, tubular atrophy and interstitial fibrosis. By immunofluorescence microscopy, there was no significant difference in the intensity of glomerular IgA staining between the two groups.

The precise quantitative analysis showed that total glomerular area and tuft area were significantly larger in group O than group N. Cell numbers per glomeruli showed no difference between the two groups. On the other hand, cell numbers divided by tuft area were significantly less in group O. The percentage of mesangial matrix area and α-SMA-positive area showed no statistical difference between the two groups.

Comparison of GBM Thickness

As shown in figure 1, each thickness of the lamina rara interna, the sum of lamina densa and lamina rara externa, and total GBM was significantly increased in group O compared with group N (29 ± 18 to 38 ± 20 nm, $p < 0.001$; 293 ± 79 to 364 ± 107 nm, $p < 0.05$; 322 ± 82 to 402 ± 100 nm, $p < 0.001$). The comparison among only male patients also revealed significantly greater GBM thickness in group O than group N (422 ± 104 to 374 ± 93 nm, $p < 0.05$). Figure 2 shows representative electron micrographs of non-obese and obese patients.

Relationship between GBM Thickness and Urinary Protein Excretion

In order to examine the relationship between GBM thickness and urinary protein excretion, Spearman correlation analysis was performed, showing a positive correlation between total GBM thickness and urinary protein excretion ($n = 74$, $rs = 0.5303$, $p < 0.0001$). Next, we examined the relationship between GBM thickness excluding lamina rara interna and urinary protein excretion because lamina rara interna can be affected by various factors such as hypertension. There was also a positive correlation between GBM thickness excluding lamina rara interna and urinary protein excretion ($n = 74$, $rs = 0.5966$, $p < 0.0001$).

Original Paper

nephron
Experimental
Nephrology

Nephron Exp Nephrol 2009;112:e81–e91
DOI: 10.1159/000224798

Received: January 16, 2008
Accepted: March 2, 2009
Published online: June 16, 2009

Lipopolysaccharide-Triggered Acute Aggravation of Mesangioproliferative Glomerulonephritis through Activation of Coagulation in a High IgA Strain of ddY Mice

Makiko Shimosawa[a] Koji Sakamoto[a] Yuki Tomari[a] Kohei Kamikado[a]
Hidetaka Otsuka[a] Ning Liu[a] Hisayo Kitamura[a] Kazuhide Uemura[a]
Fumiaki Nogaki[c] Noriko Mori[b] Eri Muso[d] Haruyoshi Yoshida[e]
Takahiko Ono[a, b]

[a]Division of Molecular Medicine, University of Shizuoka School of Pharmaceutical Sciences, [b]Department of Nephrology, Shizuoka General Hospital, Shizuoka, [c]Department of Nephrology, Shimada Municipal Hospital, Shimada, [d]Department of Nephrology, Kitano Hospital, Tazuke Kofukai Medical Research Institute, Osaka, and [e]Department of Clinical Laboratory Medicine and Nephrology, Faculty of Medical Sciences, Fukui University, Fukui, Japan

Key Words
Factor X · Factor V · Protease-activated receptor 2 · Toll-like receptor 4

Abstract
Background: The high IgA (HIGA) strain of ddY mice represents an inbred model of IgA nephropathy that shows mesangioproliferative glomerulonephritis with mesangial IgA deposition. In this study, aggravation of glomerulonephritis in HIGA mice through lipopolysaccharide (LPS)-triggered activation of coagulation was investigated. ***Methods:*** Twelve-week-old HIGA and BALB/c mice were intraperitoneally injected with LPS twice at an interval of 3 days, and kidney specimens were collected 7 days after the second LPS injection. In an intervention experiment, the factor Xa inhibitor danaparoid was injected intraperitoneally every day for 7 days after the first LPS injection. ***Results:*** LPS injection induced macrophage infiltration and cellular proliferation in the mesangium together with fibrin deposition and monocyte chemoattractant protein 1 mRNA expression, as well as antigen deposition of tissue factor, factor V, factor X, and protease-activated receptor 2. These phenomena were obvious in HIGA mice when compared to BALB/c mice. Interestingly, toll-like receptor 4 was intensely expressed in HIGA mice before LPS injection and subsequently decreased. Danaparoid treatment significantly ameliorated proteinuria, cellular proliferation, and fibrin deposition. ***Conclusions:*** The present data suggest that tissue factor and factor V induction by LPS may in part accelerate mesangioproliferative glomerulonephritis through activation of factor X and downstream proinflammatory and procoagulant mechanisms.

Introduction

IgA nephropathy is one of the most prevalent types of glomerulonephritis and shows mesangioproliferative lesions with IgA deposition. Although the cause of IgA nephropathy is unknown, immune disturbances have been suggested because of the occurrence of elevated levels of

KARGER
Fax +41 61 306 12 34
E-Mail karger@karger.ch
www.karger.com

1660–2129/09/1124–0081$26.00/0

Accessible online at:
www.karger.com/nee

Takahiko Ono, MD
Division of Molecular Medicine
University of Shizuoka School of Pharmaceutical Sciences
52-1 Yada, Suruga-ku, Shizuoka City 422-8526 (Japan)
Tel. +81 54 264 5763, Fax +81 54 264 5764, E-Mail ono@u-shizuoka-ken.ac.jp

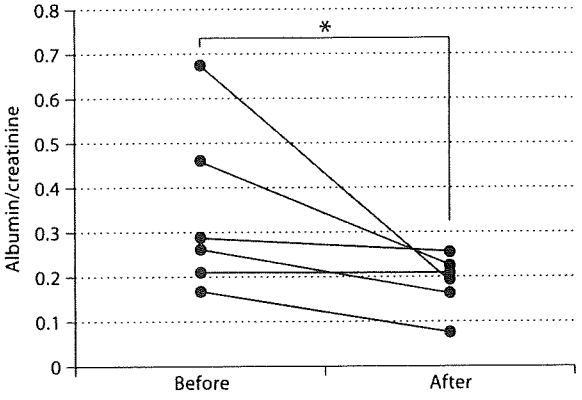

Fig. 4. Change in urinary protein after LPS administration and danaparoid treatment. Significant suppression of urinary albumin excretion by LPS + danaparoid was observed after treatment. * $p < 0.05$ versus before LPS + danaparoid injection (6 mice per group).

Effect of Danaparoid on Urinary Albumin Excretion in LPS-Injected HIGA Mice

Danaparoid treatment significantly suppressed urinary albumin excretion in LPS-injected HIGA mice (before injection, 0.35 ± 0.08; after injection of LPS + danaparoid, 0.19 ± 0.03 albumin/creatinine; $p < 0.05$; fig. 4).

Effect of Danaparoid on Histology

As shown in figure 4, a significant 21% increase in the total glomerular cell number was observed in LPS-injected BALB/c mice when compared to the basal BALB/c group. Basal HIGA mice presented a mesangial cell proliferation rate that was 30% higher than that of basal BALB/c mice. Furthermore, HIGA mice presented another 30% increase after LPS injection. This increase was significantly suppressed to basal levels by treatment with danaparoid (basal BALB/c, 38.7 ± 1.7; LPS-injected BALB/c, 46.9 ± 0.7; basal HIGA, 50.4 ± 1.5; LPS-injected HIGA, 65.4 ± 2.9; LPS + danaparoid-injected HIGA, 52.6 ± 2.0 cells/glomerular cross-section; fig. 5).

LPS injection slightly increased the number of PCNA-positive cells in the glomeruli of BALB/c mice, but significantly increased this number of HIGA mice to 2.6-fold over the basal level. Interestingly, this increase was significantly suppressed to basal levels of BALB/c mice by danaparoid treatment (basal BALB/c, 0.6 ± 0.2; LPS-injected BALB/c, 1.1 ± 0.2; basal HIGA, 0.8 ± 0.2; LPS-injected HIGA, 2.1 ± 0.3; LPS + danaparoid-injected HIGA, 0.6 ± 0.2 cells/glomerular cross-section; fig. 6).

LPS-Triggered Aggravation of Glomerular Fibrin Deposition and Suppression by Danaparoid

Immunohistochemical analysis revealed scarce fibrin deposition in basal BALB/c mice, and moderate deposits in the mesangium and partially along the capillary loops after LPS injection. Fibrin deposition was mild to moderate in basal HIGA mice, but increased 2-fold after LPS injection. Furthermore, LPS-induced fibrin deposition in HIGA mice was significantly inhibited by danaparoid treatment (basal BALB/c, 0.3 ± 0.0%; LPS-injected groups of BALB/c, 11.3 ± 2.0%; saline-injected HIGA, 6.5 ± 0.8%; LPS-injected HIGA, 13.3 ± 0.3%; LPS + danaparoid-injected HIGA, 9.3 ± 0.4% of the glomerular cross-section; fig. 7).

RT-PCR Analysis of Tissue Factor and MCP-1 mRNA in the Renal Cortex

The mRNA expression of tissue factor and MCP-1 in the renal cortex was negative in BALB/c mice, but positive in HIGA mice. LPS administration increased both mRNAs mildly in BALB/c mice, and markedly in HIGA mice. These increases were suppressed by danaparoid to the basal levels in HIGA mice (fig. 8).

Discussion

In this study, we investigated the role of coagulation in the LPS-triggered acute aggravation of MsPGN in HIGA mice. Moreover, we analyzed the effect of danaparoid as a factor Xa inhibitor on MsPGN aggravation. We found that: (1) LPS administration induced cellular proliferation and macrophage infiltration in the mesangium together with fibrin and factor X deposition, and expression of tissue factor, factor V, and PAR2 expressions; (2) these phenomena were prominent in HIGA mice when compared to BALB/c mice; (3) TLR4 expression was intense in basal HIGA mice, and decreased after LPS administration in contrast to the mild expression observed in both basal and LPS-injected BALB/c mice; (4) danaparoid treatment significantly ameliorated proteinuria, cellular proliferation, macrophage infiltration, and fibrin deposition after LPS-triggered aggravation of HIGA.

In IgA nephropathy, mesangial proliferation with mesangial matrix widening and IgA deposition is a common pathological finding [14]. Intraglomerular coagulation